

## 2.5. ELECTRON DIFFRACTION AND ELECTRON MICROSCOPY IN STRUCTURE DETERMINATION

selecting the order in which pixels enter the correction step (2) in (2.5.6.28). It was observed that if a pixel is selected such that its projection direction is perpendicular to the projection direction of the previous pixel, the convergence is achieved faster (Hamaker & Solmon, 1978; Herman & Meyer, 1993). Interestingly, a random order works almost equally well (Natterer & Wübbeling, 2001).

In single-particle reconstruction, ART has been introduced in the form of ‘ART with blobs’ (Marabini *et al.*, 1998) and is available in the *Xmipp* package (Sorzano *et al.*, 2004). In this implementation, the reconstruction structure is represented by a linear combination of spherically symmetric, smooth, spatially limited basis functions, such as Kaiser–Bessel window functions (Lewitt, 1990, 1992; Matej & Lewitt, 1996). Introduction of blobs significantly reduces the number of iterations necessary to reach an acceptable solution (Marabini *et al.*, 1998).

The major advantage of iterative reconstruction methods is the ability to take advantage of *a priori* knowledge, *i.e.*, any information about the protein structure that was not initially included in the data processing, and introduce it into the reconstruction process in the form of constraints. Examples of such constraints include similarity to the experimental (measured) data, positivity of the protein mass density (only valid in conjunction with the CTF correction), bounded spatial support *etc.* Formally, the process of enforcing selected constraints is best described in the framework of the projections onto convex sets (POCS) theory (Sezan & Stark, 1982; Youla & Webb, 1982; Sezan, 1992) introduced into EM by Carazo and co-workers (Carazo & Carrascosa, 1986, 1987; Carazo, 1992).

## 2.5.6.5. Filtered backprojection

The method of filtered backprojection (FBP) is based on inversion formulae (2.5.6.11) (in two dimensions) or (2.5.6.14) (in three dimensions). It comprises the following steps: (i) a Fourier transform of each projection is computed; (ii) Fourier transforms of projections are multiplied by filters that account for a particular distribution of projections in Fourier space; (iii) the filtered projections are inversely Fourier transformed; (iv) real-space backprojection of processed projections yields the reconstruction. The method is particularly attractive due to the fact that the reconstruction calculated using simple real-space backprojection can be made efficient if the filter function is easy to compute.

In two dimensions with uniformly distributed projections the weighting function  $c(|R|, \Psi)$  in Fourier space is the ‘ramp function’  $|R|$  [(2.5.6.13)]. In two dimensions with nonuniformly distributed projections, when the analytical form of the distribution of projections is not known, an appropriate approximation to  $c(|R|, \Psi)$  has to be found. A good choice is to select weights such that the backprojection integral becomes approximated by a Riemann sum (Penczek *et al.*, 1996),

$$\begin{aligned} c(|R|, \Psi) = |R| \, dR \, d\Psi \rightarrow c(R_j, \Psi_i) &= R_j \frac{1}{2\pi} \frac{\Psi_{i+1} - \Psi_{i-1}}{2} \\ &= R_j \frac{\Delta\Psi_i}{4\pi}. \end{aligned} \quad (2.5.6.29)$$

For a given set of angles the weights  $c(R_j, \Psi_i)$  are easily computed (Fig. 2.5.6.5).

In three dimensions, the weighting (2.5.6.29) is applicable in a single-axis tilt data-collection geometry, where the 3D reconstruction can be calculated as a series of independent 2D reconstructions. In the general 3D case, the analogue of weighting (2.5.6.29) cannot be used, as the data are given in the form of 2D projections and it is not immediately apparent what fraction of the 3D Fourier volume is occupied by Fourier pixels in projections. However, the analogue of weighting (2.5.6.29) can be used in the inversion of 3D Radon transforms or in a direction

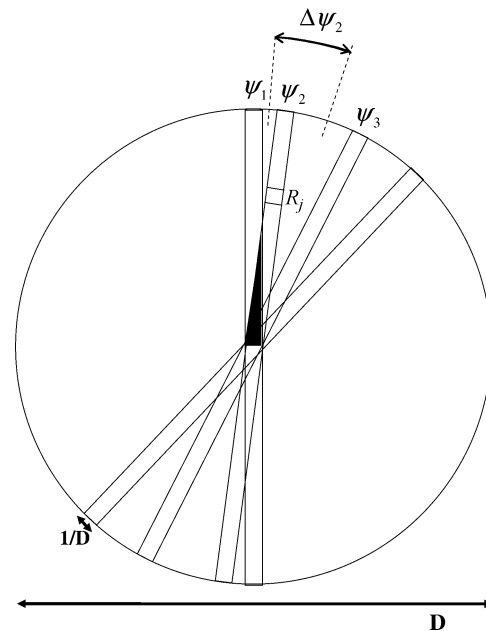


Fig. 2.5.6.5. Nonuniform distribution of projections. The projection weights for the reconstruction algorithms are chosen such that the backprojection integral becomes approximated by a Riemann sum and are equal to the angular length of an arc  $\Delta\Psi_i$  (2.5.6.29). In Fourier space, projections of an object with real-space radius  $D$  form rectangles with width  $1/D$ . In the exact filter backprojection reconstruction method, the weights are derived based on the amount the overlap between projections (2.5.6.29).

inversion of 3D ray transforms that is based on an intermediate step of converting 2D projection data to 1D projection data, as described in Section 2.5.6.6.

In order to arrive at a workable solution, the weighting functions applicable to 2D projections are constructed based on an explicitly or implicitly formulated concept of the ‘local density’ of projections. This concept was introduced by Bracewell (Bracewell & Riddle, 1967), who suggested for a 2D case of nonuniformly distributed projections a heuristic weighting function,

$$c(R_j, \Psi_i) = \frac{R_j}{\sum_l \exp[-\text{constant}(|\Psi_i - \Psi_l| \bmod \pi)^2]}. \quad (2.5.6.30)$$

The weighting function (2.5.6.30) can be easily extended to three dimensions; however, it has a major disadvantage that for a uniform distribution of projections it does not approximate well the weighting function (2.5.6.29), which we consider optimal.

Radermacher *et al.* (1986) proposed a derivation of a general weighting function using a deconvolution kernel calculated for a given (nonuniform) distribution of projections and, in modification of (2.5.6.14), a finite length of backprojection (Fig. 2.5.6.3). Such a ‘truncated’ backprojection is

$$\hat{b}_i(\mathbf{r}) = \varphi_2(\mathbf{x}_\tau) * l(\mathbf{r}), \quad \boldsymbol{\tau} \perp \mathbf{x} \quad (2.5.6.31)$$

with projection directions  $\boldsymbol{\tau}(\theta, \psi)_i$  and

$$\begin{aligned} l(\mathbf{r}) &= \delta(\mathbf{x}_\tau) t(z_\tau), \\ t(z_\tau) &= \begin{cases} 1 & -(D/2) \leq z \leq (D/2), \\ 0 & \text{otherwise,} \end{cases} \end{aligned} \quad (2.5.6.32)$$

where  $D$  is the diameter of the object or the length of the backprojection  $l$ . By taking the Fourier transform of (2.5.6.31) and using the central section theorem (2.5.6.8), we obtain a 3D Fourier transform of the backprojected projection,

## 2. RECIPROCAL SPACE IN CRYSTAL-STRUCTURE DETERMINATION

$$\Phi_3(u, v, w) = \Phi_2(\mathbf{u}_\tau) D \operatorname{sinc}(D\pi w_\tau), \quad (2.5.6.33)$$

and the 3D reconstruction is obtained by the inverse Fourier transform of the sum of contributions given by (2.5.6.33),

$$\mathcal{F}[\hat{\mathbf{b}}(\mathbf{r})] = \sum_i \Phi_2(\mathbf{u}_\tau) D \operatorname{sinc}(D\pi w_\tau). \quad (2.5.6.34)$$

$z_\tau$  and  $w_\tau$  are variables in real and Fourier spaces, respectively, both extending in the direction of the projection direction  $\tau(\theta, \psi)_i$ .

In this analysis, the transfer function of the backprojection algorithm is obtained by setting  $\Phi_2(\mathbf{u}_\tau) = 1$ , that is by finding the response of the algorithm to the input composed of delta functions in real space. This yields the inversion formula for a general weighted backprojection algorithm:

$$\varphi_3(\mathbf{r}) = \mathcal{F}[\hat{\mathbf{b}}(\mathbf{r})]c(u, v, w), \quad (2.5.6.35)$$

with the weighting function given by

$$c(u, v, w) = \frac{1}{\sum_i D \operatorname{sinc}(D\pi w_\tau)}. \quad (2.5.6.36)$$

The general weighting function (2.5.6.36) is consistent with analytical solutions (2.5.6.11) and (2.5.6.14), as it can be shown that by assuming infinite support ( $D \rightarrow \infty$ ) and continuous and uniform distribution of projection directions, in two dimensions one obtains  $c(u, v) = (u^2 + v^2)^{-1/2}$  (Radermacher, 2000).

The derivation of (2.5.6.36) is based on the analysis of continuous functions and its direct application to discrete data results in reconstruction artifacts; therefore, Radermacher (1992) proposed attenuating the sinc functions in (2.5.6.36) by exponent functions with decay depending on the diameter of the structure  $D$ , or simply replacing the sinc functions by exponent functions. This, however, reduces the concept of the weighting function corresponding to the deconvolution to the concept of the weighting function representing the ‘local density’ of projections (2.5.6.30). The general weighted backprojection reconstruction is implemented in *SPIDER* (using exponent-based weighting functions) (Frank *et al.*, 1996), *Xmipp* (Sorzano *et al.*, 2004) and *SPARX* (Hohn *et al.*, 2007).

Harauz & van Heel (1986) proposed basing the calculation of the density of projections, thus the weighting function, on the overlap of Fourier transforms of projections in Fourier space. Although the concept is general, it can be easily approached in two dimensions. If the diameter of the object is  $D$ , the width of a Fourier transform of a projection is  $2/D$  (Fig. 2.5.6.5), as follows from the central section theorem (2.5.6.8). Harauz and van Heel postulated that the weighting should be inversely proportional to the sum of geometrical overlaps between a given central section and the remaining central sections. For a pair of projections  $il$ , this overlap is

$$o_{il}(R) = T[DR \sin(\Psi_i - \Psi_l)], \quad (2.5.6.37)$$

where  $T$  represents the triangle function (selected by the authors because it can be calculated efficiently). Also, owing to the Friedel symmetry of central sections, the angles in (2.5.6.37) are restricted such that  $0 \leq \Psi_i - \Psi_l \leq (\pi/2)$ . In this formulation, the overlap is limited to the maximum frequency,

$$R_{il}^{\max} = \frac{2}{D \sin(\Psi_i - \Psi_l)}. \quad (2.5.6.38)$$

Thus, the overlap function becomes

$$o_{il}(R) = \begin{cases} 1 - (R/R_{il}^{\max}) & 0 \leq R < u_{il}^{\max} \\ 0 & R > u_{il}^{\max} \end{cases}. \quad (2.5.6.39)$$

In effect, the weighting function, called by the authors an ‘exact filter’, is

$$c(R, \Psi_i) = \frac{1}{1 + \sum_{l, l \neq i} o_{il}(R)}. \quad (2.5.6.40)$$

The weighting function (2.5.6.40) easily extends to three dimensions; however, the calculation of the overlap between central sections in three dimensions (represented by slabs) is more elaborate (Harauz & van Heel, 1986). The method is conceptually simple and computationally efficient. However, (2.5.6.40) does not approximate the correct weighting well for a uniform distribution of projections [*i.e.*, it should yield  $c(R, \Psi_i) = R$ ]. This, as can be seen by integrating (2.5.6.39) over the whole angular range, is not the case. The exact filter backprojection reconstruction is implemented in the *IMAGIC* (van Heel *et al.*, 1996), *SPIDER* (Frank *et al.*, 1996) and *SPARX* (Hohn *et al.*, 2007) packages.

The 3D reconstruction methods based on filtered backprojection are commonly used in single-particle reconstruction. The reasons are: their versatility, ease of implementation, and – in comparison with iterative methods – good computational efficiency. Unlike in iterative methods, there are no parameters to adjust, although it has been noted that the results depend on the value of the diameter  $D$  of the structure in all three weighting functions [(2.5.6.30), (2.5.6.36) and (2.5.6.38)], so the performance of the reconstruction algorithm can be optimized for a particular data-collection geometry by changing the value of  $D$  (Paul *et al.*, 2004). However, because computation of the weighting function involves calculation of pairwise distances between projections, the computational complexity is proportional to the square of the number of projections and for large data sets these methods become inefficient. It also has to be noted that the weighting functions (2.5.6.30), (2.5.6.36) and (2.5.6.40) remain approximations of the correct weighting function (2.5.6.29).

### 2.5.6.6. Direct Fourier inversion

Direct Fourier methods are based on the central section theorem (2.5.6.8). A set of the 2D Fourier transforms of projections yields an approximation to  $\Phi_3$  on a nonuniform 3D grid, and a subsequent numerical 3D inverse Fourier transform gives an approximation to  $\varphi_3$ . If the 3D inverse Fourier transform could be realized by means of the 3D inverse fast Fourier transform (FFT), one would have a very fast reconstruction algorithm. Unfortunately, the preprocessing step yields  $\Phi_3$  on a nonuniform grid. In effect, the 3D inverse FFT is not applicable and an additional step of recovering samples of  $\Phi_3$  on a uniform grid from the available samples on a nonuniform grid is necessary.

One possibility is to resample the nonuniformly sampled version of  $\Phi_3$  onto a 3D Cartesian grid by some form of interpolation. For example, Grigorieff used a modified trilinear interpolation scheme in the *FREALIGN* package (Grigorieff, 1998). Simple interpolation methods have been found to give inaccurate results, although more sophisticated interpolation schemes can go a long way to improve the accuracy (Lanza-